

Rossella Arrigo, Rosalia Teresi and Nadka Tzankova Dintcheva\*

# Mechanical and rheological properties of polystyrene-*block*-polybutadiene-*block*-polystyrene copolymer reinforced with carbon nanotubes: effect of processing conditions

DOI 10.1515/polyeng-2016-0455

Received December 21, 2016; accepted March 4, 2017

**Abstract:** Styrene-*b*-butadiene-*b*-styrene (SBS)-based nanocomposites filled with unmodified and –COOH functionalized carbon nanotubes (CNTs) have been formulated at different processing conditions in order to provide an understanding of the influence of the processing temperature and mixing speed on the nanofillers dispersion and on the overall properties of the nanocomposites. The evaluation of the nanocomposites' mechanical and rheological behavior reveals that the effect of the processing speed on the final properties is almost negligible. Differently, the processing temperature influences strongly the mechanical and rheological properties of SBS-based nanocomposites. Indeed, for the nanocomposites formulated at high temperatures a significant enhancement of the overall properties with respect to the neat matrix has been achieved. Moreover, morphological analyses show that the state of dispersion of both unmodified and functionalized CNTs progressively improves as the processing temperature increases. Particularly, at low processing temperatures a segregated morphology in which the nanofillers are selectively confined in the domains of the SBS matrix has been obtained, while the nanocomposites formulated at 180°C show a homogeneous and uniform CNTs dispersion throughout the matrix and a strong level of interfacial adhesion between the copolymer chains and the dispersed nanofillers.

**Keywords:** carbon nanotubes (CNTs); mechanical properties; polystyrene-*block*-polybutadiene-*block*-polystyrene; processing conditions; rheological behavior.

## 1 Introduction

Styrene-*b*-butadiene-*b*-styrene (SBS) is a thermoplastic elastomer with many commercial applications, as it combines the mechanical properties of rubbers with the easy processability of thermoplastics [1–3]. Moreover, the modification of the composition, in terms of styrene/butadiene ratio, and of the chain architecture allows to obtain a final material with tailorable mechanical properties [4]. In SBS, at room temperature, the rubbery polybutadiene segments are linked to the glassy polystyrene blocks; depending on the molecular weight of the blocks and of the relative length of segments, this copolymer can lead to a microphase separation into soft and hard domains, resulting in the formation of spherical, cylindrical, or lamellar morphologies [5–7]. Interestingly, the microstructure of polystyrene and polybutadiene segments and the orientation of formed domains strongly influence the deformation behavior of SBS [8, 9].

Recently, many studies devoted to the expansion of SBS field of application through the incorporation of various fillers have been performed [10–12]. Due to the multi-phase nature of SBS, solid particles of different shape and dimensions can be selectively confined into copolymer domains, offering the possibility to control the spatial distribution of the fillers within copolymer matrix [13–15]. Thereby, the final properties of the resulting nanocomposite can be properly optimized and tailored for a specific application [16]. For instance, the selective confinement of carbon nanotubes (CNTs) into polystyrene domains of a polystyrene-*b*-polyisoprene copolymer has been exploited to control the dispersion and orientation of the used nanofillers, allowing for the fabrication of a nanocomposite with desirable morphology and nanoparticle alignment [17].

Carbon nanotubes are one of the most promising candidates for the formulation of innovative SBS-based nanocomposites, due to their unique combination of mechanical, electrical, and magnetic properties [18–20]. Besides, the asymmetric shape of CNTs makes them

\*Corresponding author: Nadka Tzankova Dintcheva, Dipartimento di Ingegneria Civile, Ambientale, Aerospaziale, dei Materiali, Università di Palermo, Viale delle Scienze, Ed. 6, 90128 Palermo, Italy, e-mail: nadka.dintcheva@unipa.it

Rossella Arrigo and Rosalia Teresi: Dipartimento di Ingegneria Civile, Ambientale, Aerospaziale, dei Materiali, Università di Palermo, Viale delle Scienze, Ed. 6, 90128 Palermo, Italy

particularly interesting for the formulation of engineering materials with enhanced anisotropic properties, such as electrical and thermal conductivity and so on [21]. Nevertheless, due to Van der Waals interactions, CNTs show a strong tendency to agglomerate and the formed bundles, acting as defects in the host matrix, cause worsening of the mechanical properties [22, 23]. Furthermore, due to the poor compatibility between CNTs and polymer, a weak level of interfacial bonding is reached; as a consequence, the effectiveness of the load transfer from polymer to nanofillers is compromised [24]. To overcome the disadvantages related to the poor dispersion of CNTs in polymers, different strategies have been pursued, among other high shear mixing [25], adding of surfactants or dispersing agents [26] and chemical functionalization of CNTs surface [10, 27, 28]. An interesting work by Wang et al. [29] reports the grafting of SBS onto multi-walled CNTs and the introduction of the so-formulated nanoparticles in SBS copolymer. The resulting nanocomposite shows improved mechanical properties and electrical conductivity due to the obtained uniform dispersion of functionalized CNTs within matrix and excellent interfacial adhesion.

The work presented here aims to provide an understanding of the influence of the processing parameters on the dispersion of CNTs in SBS copolymer. For this purpose, SBS-based nanocomposites containing unmodified and -COOH functionalized CNTs have been formulated through melt-mixing at different temperatures and mixing speeds. The mechanical behavior, rheology, and morphology of resulting nanocomposites have been evaluated and discussed, considering the effect of the processing conditions and of the CNTs surface functionalization as well.

## 2 Materials and methods

### 2.1 Materials

The materials used in this work were:

- Styrene-*b*-butadiene-*b*-styrene copolymer (SBS), with styrene content at 30 wt%, purchased by Sigma-Aldrich (Saint-Louis, MO, USA). The main properties of used SBS are listed in Table 1.
- Bare multiwalled CNTs, purchased by Cheap Tubes (Grafton, VT, USA); main properties: OD = 120 ÷ 180 nm, ID = 10 ÷ 20 nm,  $L = 10 \div 20 \mu\text{m}$ , purity >95 wt%, ash <1.5 wt%, specific surface area SSA >40 m<sup>2</sup>/g, and electrical conductivity EC >10<sup>-2</sup> S/cm.
- Multiwalled CNTs containing ~1 wt% of covalently linked -COOH groups (COOH-CNTs), purchased by

**Table 1:** Inherent properties of used SBS.

Molecular weight	~140.000 (determined by GPC)
Composition	Styrene 30 wt%
Intrinsic viscosity	1.0
Density	0.94 g/ml at 25°C
Elastic modulus	~250 MPa
Tensile strength	~4.5 MPa

GPC, gel permeation chromatography.

Cheap Tubes, USA; main properties: outer diameter OD = 120 ÷ 180 nm, inner diameter ID = 10 ÷ 20 nm, length  $L = 10 \div 20 \mu\text{m}$ , purity >95 wt%, ash <1.5 wt%, specific surface area SSA >60 m<sup>2</sup>/g, and electrical conductivity EC >10<sup>-2</sup> S/cm.

### 2.2 Processing

The preparation of SBS/CNTs and SBS/COOH-CNTs nanocomposites was carried out using a Brabender mixer (Duisburg, Germany) at three different temperatures, particularly at 120°C, 150°C and 180°C, and 50 rpm for 5 min. In order to evaluate the effect of the mixing speed, the nanocomposite SBS/COOH-CNTs obtained at 180°C was prepared at two different processing speeds, namely 50 and 100 rpm. The nanotubes were added at 3 wt% into the melted matrix after 2 min of processing. The chosen CNTs content ensures significant improvement of mechanical properties, avoiding re-aggregation phenomena of CNTs. The pristine SBS copolymer was subjected to the same processing.

The SBS and SBS-based nanocomposite specimens used for different characterizations were prepared by a compression molding step, using a Carver Press (Wabash, IN, USA) at the same processing temperature, for 5 min, under a pressure of about 30 MPa.

### 2.3 Characterizations

Rheological tests were performed using a strain-controlled rheometer (mod. ARES G2 by TA Instrument, New Castle, DE, USA) in parallel plate geometry (plate diameter 25 mm). The complex viscosity ( $\eta^*$ ) and storage ( $G'$ ) and loss ( $G''$ ) moduli were measured performing frequency scans from  $\omega = 10^{-2}$  to 10<sup>2</sup> rad/s at same processing temperatures. The strain amplitude was  $\gamma = 2\%$ , which preliminary strain sweep experiments proved to be low enough to be in the linear viscoelastic regime.

Mechanical tests of the samples were carried out using a universal Instron machine (model 3365, High

Wycombe, UK), according to ASTM D882 (crosshead speed of 100 mm/min). The average values for elongation at break, EB, and for elastic modulus,  $E$ , were calculated and the standard deviation is reported in the figures.

Dynamic mechanical thermal analysis (DMTA) was performed using a Rheometrics DMTA V instrument (Piscataway, NJ, USA) in round shear sandwich mode. The tests have been carried out using a temperature sweep method, between 30°C and 140°C at a heating rate of 5°C/min. The frequency was set to 1 Hz and the maximum strain amplitude was 2%. The storage modulus ( $G'$ ) and the damping factor ( $\tan \delta$ ) as a function of the temperature have been recorded.

Differential scanning calorimetry (DSC) was performed using a DSC 60 Shimadzu calorimeter (Kioto, Japan). All experiments were run with samples of about 10 mg in 40  $\mu$ l sealed aluminum pans. The calorimetric scan (−110°C–105°C) was performed for each sample at a heating rate of 10°C/min.

The dispersion of CNTs in SBS matrix has been evaluated through scanning electron microscopy (SEM) observations, performed on nitrogen-fractured radial surfaces of the investigated samples with a Philips ESEM XL30 microscope (Eindhoven, The Netherlands) and transmission electron microscopy (TEM) with a Jeol JEM-2100 (Akishima, Japan) at 200 kV, on ultrathin films with thickness of about 100 nm, prepared via cutting from specimens block with a Leica Ultramicrotome EMUC6.

## 3 Results and discussion

### 3.1 Effect of the processing temperature

Rheological analyses can provide useful information about the state of dispersion of nanoparticles within host polymer matrix [30]; furthermore, the assessment of the rheological behavior allows to evaluate the effect of the processing parameters on the internal structure of the nanocomposites. In Figure 1, the complex viscosity ( $\eta^*$ ) and the storage ( $G'$ ) and loss ( $G''$ ) moduli as a function of frequency for neat SBS and SBS-based nanocomposites formulated at different processing temperatures are reported. It can be observed that, as the processing temperature increases, the difference between the rheological behavior of the nanocomposites and that of the neat matrix becomes more pronounced. Indeed, for the systems formulated at 120°C and 150°C the complex viscosity and moduli values of the nanocomposites are quite similar to those of neat SBS copolymer, and no variation of the rheological behavior

attributable to the CNTs presence can be detected. These features seem to indicate a poor dispersion of CNTs in these systems [31]. Differently, the nanocomposites formulated at 180°C show higher complex viscosity and moduli values than those of neat SBS in the whole investigated frequency range, and this behavior is more pronounced for COOH–CNTs containing nanocomposite. The last can be understood considering that the functionalization of CNTs with carboxylic groups enhances the affinity between matrix and nanofillers, improving the dispersion of CNTs within SBS copolymer. Additionally, the disappearance of the Newtonian plateau for nanocomposites containing both unmodified and –COOH functionalized CNTs can be noticed. The obtained results suggest that the processing of the nanocomposites at 180°C leads to the obtainment of a more uniform and homogeneous distribution of nanofillers within host matrix with respect to the nanocomposites obtained at lower processing temperatures. Additionally, the differences in the rheological behavior between the systems formulated at different temperatures could be explained considering some modification of the internal structure of the neat SBS copolymer. Indeed, it is well known that in block copolymers, as a function of the processing temperature, modifications of the internal microstructure can occur and different morphologies and orientation of the domains can be obtained [32, 33].

In Figure 2, the main mechanical properties, e.g. elastic modulus ( $E$ ), tensile strength (TS), and elongation at break (EB) for neat matrix and nanocomposites formulated at different temperatures are reported. Concerning the mechanical behavior of neat SBS copolymer, a progressive increase of  $E$  and a decrease of EB can be observed with an increase of processing temperature; differently, the TS values seem to be almost unaffected by the processing temperature. As discussed earlier, this behavior could be attributed to the variation of the internal microstructure of SBS copolymer as a function of temperature [32, 33].

Let us now consider the effect of the nanofillers addition. Irrespective of the processing temperature, the presence of CNTs causes the increase of the elastic modulus and the decrease of the elongation at break, indicating that the nanocomposite rigidity is improved as a result of the nanofillers addition while the nanocomposites become somewhat brittle compared to neat SBS. The presence of –COOH functionalized CNTs leads to the obtainment of superior tensile properties with respect to unmodified CNTs-containing nanocomposite. The last can be understood considering that the presence of functional groups onto the CNTs surface enhances the interfacial adhesion between macromolecular chains and dispersed nanoparticles, promoting in this way the stress transfer across the interface.

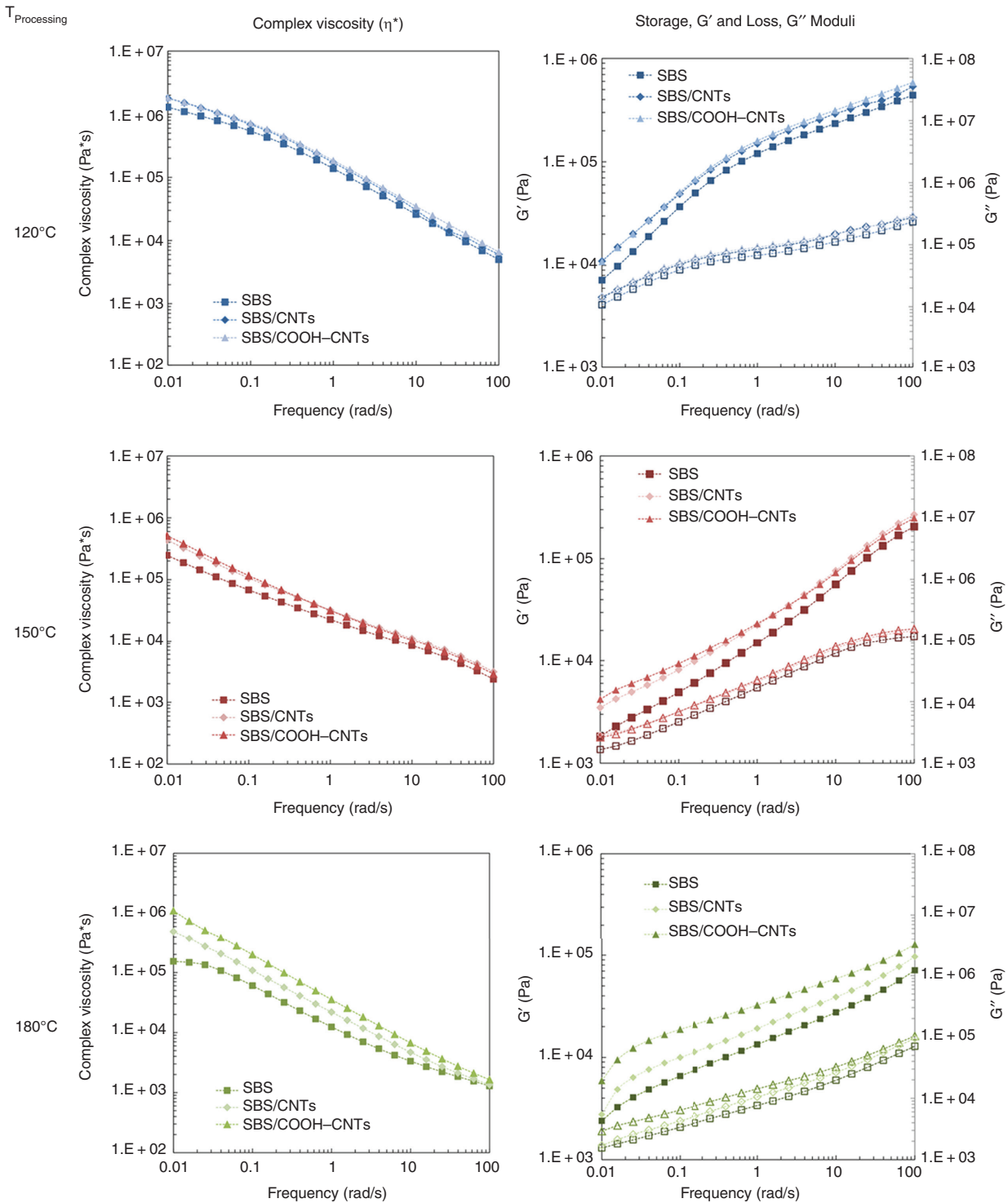


**Figure 1:** Complex viscosity and storage (full symbols) and loss (empty symbols) moduli as a function of frequency for neat SBS and SBS-based nanocomposites at different processing temperatures.

As already noticed in the analysis of the rheological behavior, the differences between nanocomposites and neat matrix become more pronounced as the processing temperature increases. For instance, the elastic modulus of SBS/COOH-CNTs nanocomposites formulated at 120°C

and 180°C increases by 9.5% and 37%, respectively, compared to the neat matrix obtained at the same temperatures. The obtained results suggest that the increase of the processing temperature has a beneficial effect on the dispersion of nanofillers, as the improved mechanical

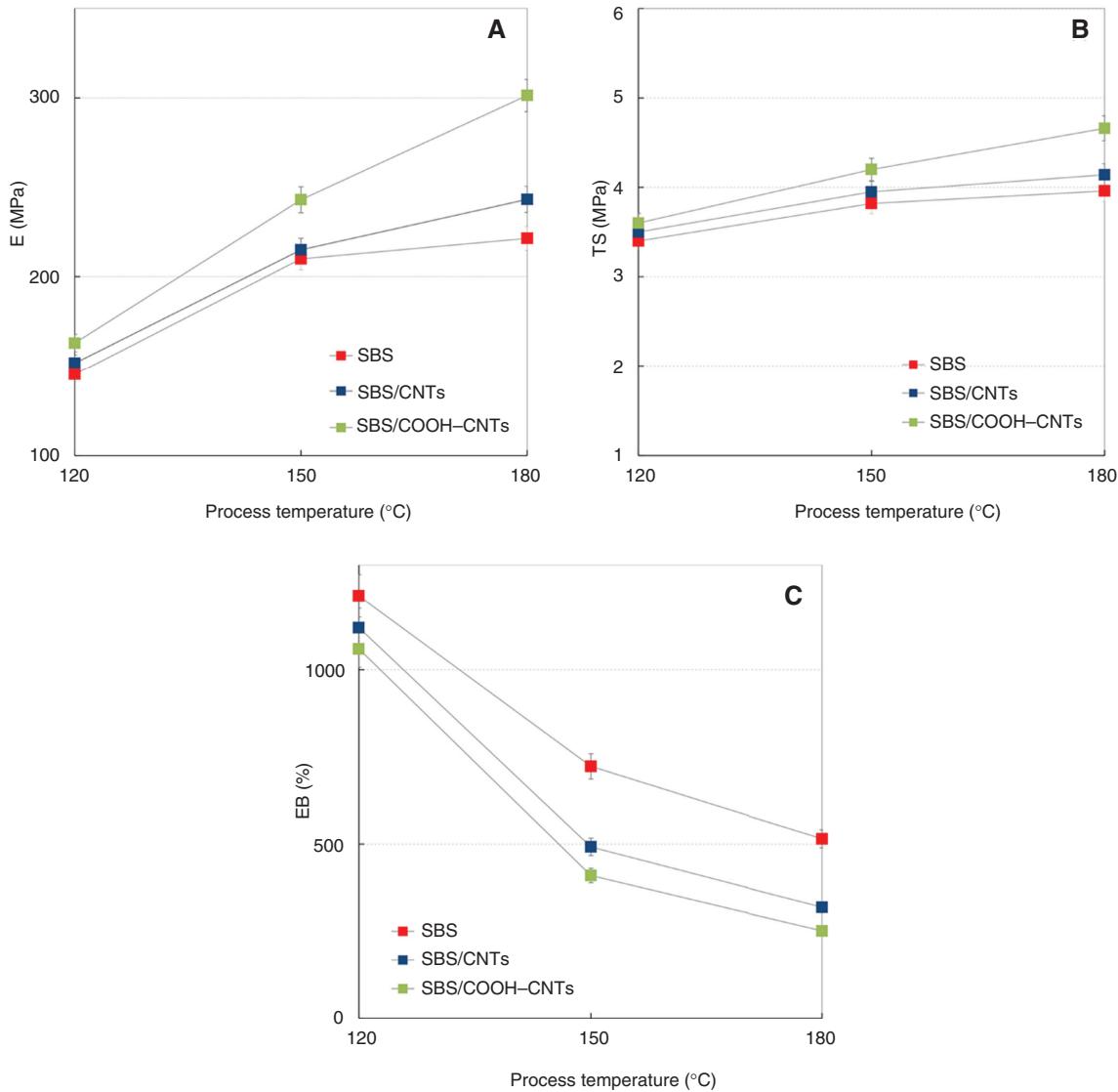


**Figure 2:** Main mechanical properties for neat SBS and SBS-based nanocomposites: (A) elastic modulus, (B) tensile strength, and (C) elongation at break as a function of processing temperature.

properties showed by nanocomposites formulated at 180°C are consistent with the achievement of a more finely and uniform dispersion of CNTs throughout the copolymer matrix.

To deeply investigate the mechanical behavior of SBS-based nanocomposites, dynamical-mechanical tests have been carried out in the viscoelastic region. In Figure 3, the trends of dynamic storage modulus ( $G'$ ) and damping factor ( $\tan \delta$ ) as a function of temperature are reported, for neat SBS and CNTs-containing nanocomposites obtained at three different processing temperatures. All investigated systems show a sudden fall in the storage modulus at a temperature around 100°C corresponding to a relaxation process involving the polystyrene domains [34]. Once again, the CNTs addition results in significant variation of

the SBS mechanical behavior solely for the nanocomposites formulated at 180°C, for which an increase of the  $G'$  value in the whole investigated temperature range corresponding to an increase of the nanocomposite rigidity can be observed. This increase is exacerbated for the nanocomposite containing COOH-CNTs, due to the presence of functional groups that improve the compatibility between nanoparticles and SBS chains, enhancing the interfacial adhesion and the nanoparticles distribution. Differently, the nanocomposites obtained at lower temperatures show a  $G'$  trend as a function of temperature similar to that of neat matrix.

In correspondence of the relaxation process recognized in  $G'$  trend, a well-distinguished maximum in the  $\tan \delta$  curve can be observed, related to the glass transition

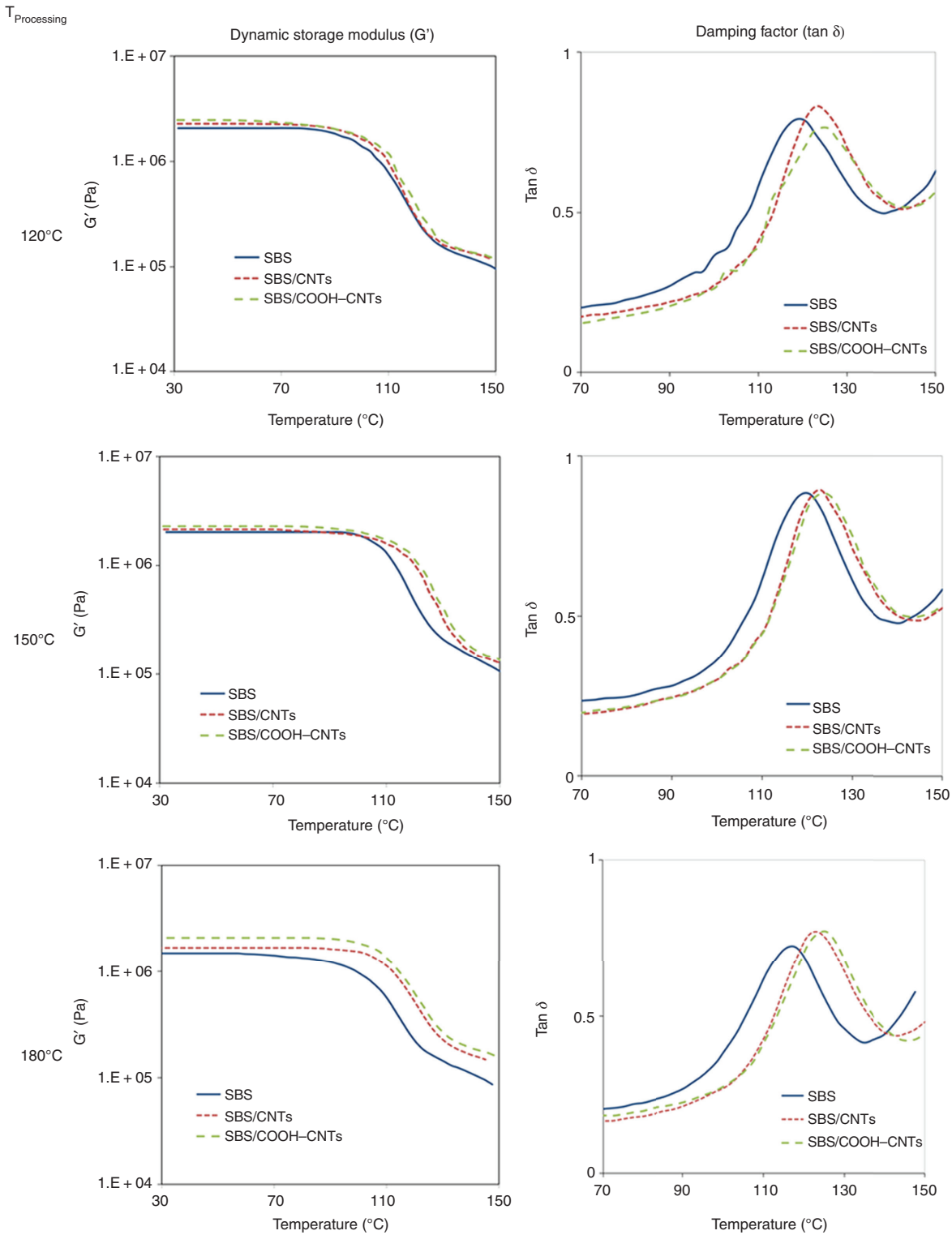


**Figure 3:** Dynamic storage modulus and damping factor for neat SBS and SBS-based nanocomposites obtained at different processing temperatures.

of polystyrene portion [34]. Regardless of processing temperature, the addition of CNTs and, even more, of COOH-CNTs causes a shift of  $\tan \delta$  peak toward higher

temperatures, indicating the loss of macromolecular mobility of SBS chains. The presence of CNTs, indeed, hinders the local motion of copolymer chains [35] and

induces a lowering of the viscous energy associated with the macromolecular motions, leading to an increase of the SBS glass transition temperature.

To better evaluate the effect of the processing temperature and of the CNTs adding on the glass transition temperature ( $T_g$ ) of SBS copolymer, DSC analyses have been carried out and the obtained results have been listed in Table 2 (Mixing speed 50 rpm). Furthermore, in Figure 4 the thermograms collected during the heating scan for neat SBS and SBS-based nanocomposites processed at 180°C are reported. Neat SBS, irrespective of the

**Table 2:** DSC data for neat SBS and SBS-based nanocomposites obtained at different (A) processing temperatures and (B) mixing speed.

Sample	$T_{g_{PB}}$ (°C)	$T_{g_{PS}}$ (°C)
(A) Mixing speed 50 rpm		
SBS – 120°C	–94.5	74.0
SBS – 150°C	–95.1	74.5
SBS – 180°C	–95.2	74.2
SBS/CNTs – 120°C	–92.1	75.3
SBS/CNTs – 150°C	–92.7	75.3
SBS/CNTs – 180°C	–93.6	75.1
SBS/COOH–CNTs – 120°C	–91.4	75.4
SBS/COOH–CNTs – 150°C	–92.2	75.7
SBS/COOH–CNTs – 180°C	–92.7	75.6
(B) Processing temperature 180°C, mixing speed 100 rpm		
SBS	–95.0	74.0
SBS/COOH–CNTs	–93.1	76.0

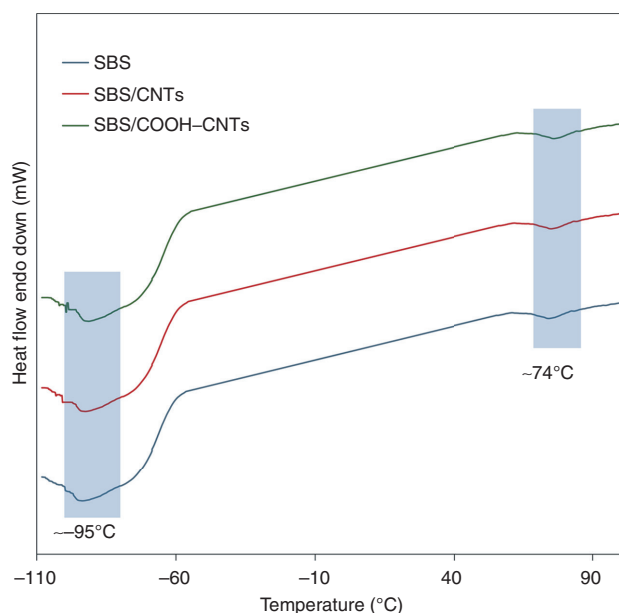


**Figure 4:** DSC thermograms for neat SBS and SBS-based nanocomposites processed at 180°C.

processing temperature, shows two different endothermic peaks: one at about  $-95^{\circ}\text{C}$ , which corresponds to the  $T_g$  of polybutadiene domains, and one at about  $74^{\circ}\text{C}$ , related to the  $T_g$  of the polystyrene phase. The addition of bare and functionalized CNTs leads to an increase of both  $T_g$  values, because of the decreased mobility of SBS macromolecules induced by the CNTs presence, as already inferred from the analysis of nanocomposites thermo-mechanical properties.

The SEM micrographs of fracture surface of SBS-based nanocomposites prepared at three different processing temperatures are shown in Figure 5. It is evident that in the nanocomposites formulated at  $120^{\circ}\text{C}$  and  $150^{\circ}\text{C}$  a poor dispersion of CNTs has been achieved. Indeed, the presence of nanofillers agglomerates can be noticed in both unmodified and functionalized CNTs-containing systems, although in the SBS/COOH–CNTs nanocomposites a more regular morphology is noticeable. It seems that, due to the improper processing temperature, the nanofillers are selectively segregated in the polybutadiene and/or polystyrene domains of the SBS matrix. Otherwise, the nanocomposites formulated at  $180^{\circ}\text{C}$  show a homogeneous and uniform dispersion of the nanofillers within the host matrix; moreover, the lack of CNTs pulled-out from the matrix indicates the strong level of interfacial adhesion reached in the SBS-based nanocomposites obtained at  $180^{\circ}\text{C}$ . To better evaluate the morphology of the SBS-based nanocomposites processed at  $180^{\circ}\text{C}$ , TEM analysis has been performed, see micrographs reported in Figure 6. As already inferred from the analysis of SEM results, both bare and COOH-functionalized CNTs are uniformly distributed within SBS host matrix, indicating that the process at higher temperature is effective in the enhancement of the nanofillers dispersion.

### 3.2 Effect of the mixing speed

In order to evaluate the effect of the mixing speed on the final properties of SBS-based nanocomposites, the processing of neat SBS and SBS/COOH–CNTs nanocomposites obtained at  $180^{\circ}\text{C}$  has been carried out at 50 and 100 rpm. In Figure 7, the complex viscosity curves and the trends of  $G'$  and  $G''$  moduli as a function of frequency are reported. It can be clearly observed that the mixing speed has a negligible effect on the rheological function of both neat SBS and COOH–CNTs-containing nanocomposite. Indeed, either the complex viscosity curves or the moduli trends of SBS-based systems obtained at 50 and 100 rpm are almost coincident, highlighting that the mixing speed

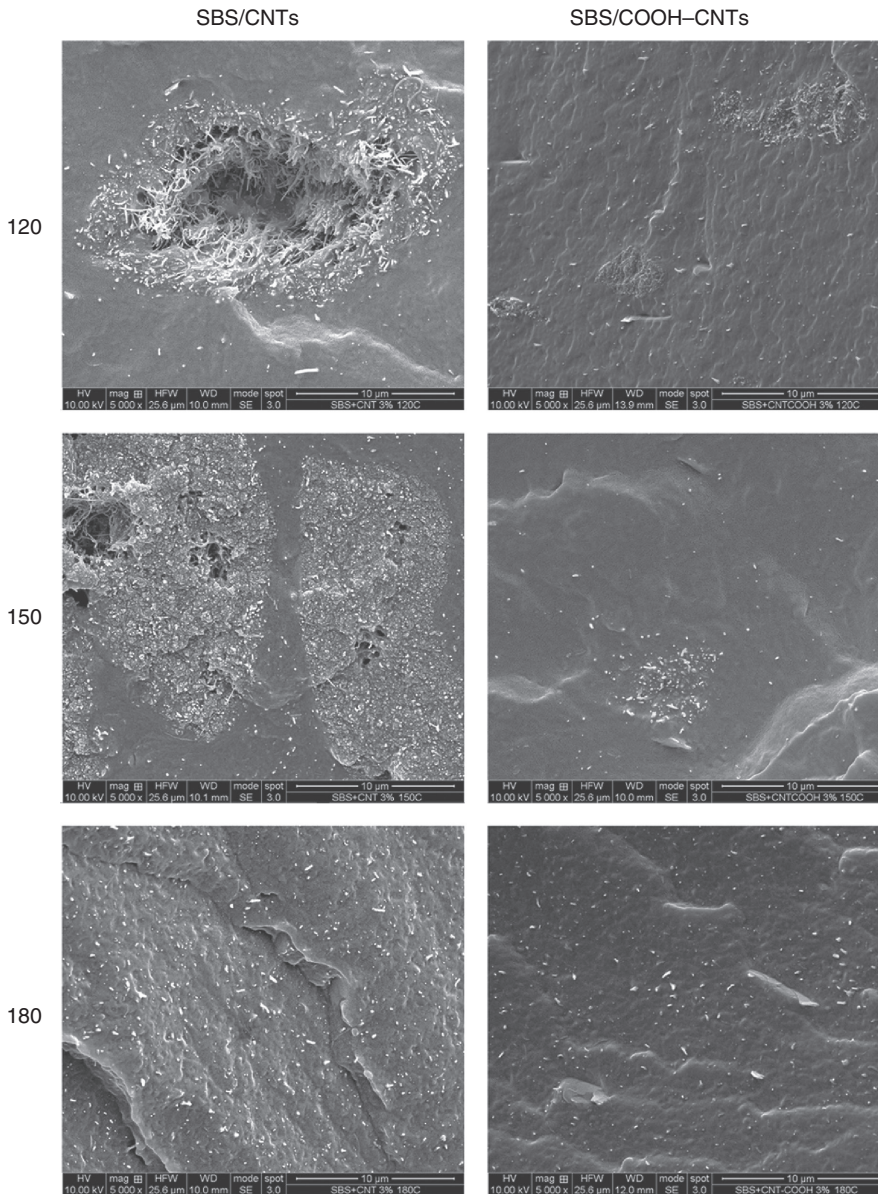


**Figure 5:** SEM micrographs of all investigated SBS-based nanocomposites.

is not the determinant in the modification of the rheological behavior of the investigated systems.

Similarly, the mechanical behavior of neat SBS and SBS/COOH-CNTs nanocomposites is slightly affected by the mixing speed. In Figure 8A–C, the values of  $E$ ,  $TS$ , and  $EB$  for the two systems processed at 50 and 100 rpm are reported. It can be noticed that the values of the mechanical properties for the neat matrix obtained at 100 rpm are scarcely lower than those showed by SBS processed at low mixing speed, suggesting that the neat matrix can experience thermo-mechanical degradation at such high mixing speed. Concerning the mechanical properties of

COOH-CNTs-containing nanocomposite, the increase of the mixing speed causes the enhancement of  $E$  and  $TS$  and a decrease of  $EB$ , highlighting that the processing at high mixing speed promotes a more uniform dispersion of CNTs within host matrix.

The same conclusions can be drawn from the analysis of the thermo-mechanical behavior of neat SBS and COOH-CNTs-based nanocomposite as reported in Figure 8D. Looking at the trends of the dynamic elastic modulus as a function of the temperature for neat SBS and CNTs-COOH-containing nanocomposite, a decrease of  $G'$  for SBS and an increase of the modulus values for

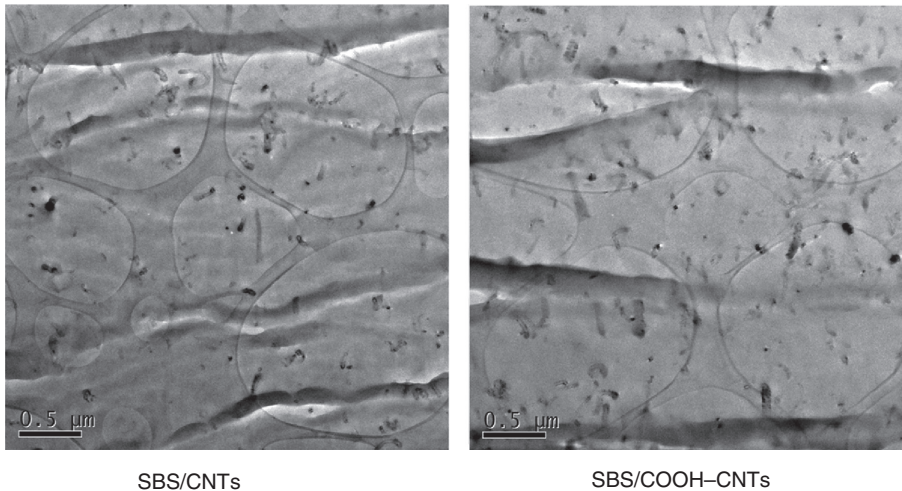


Figure 6: TEM micrographs of nanocomposites processed at 180°C.

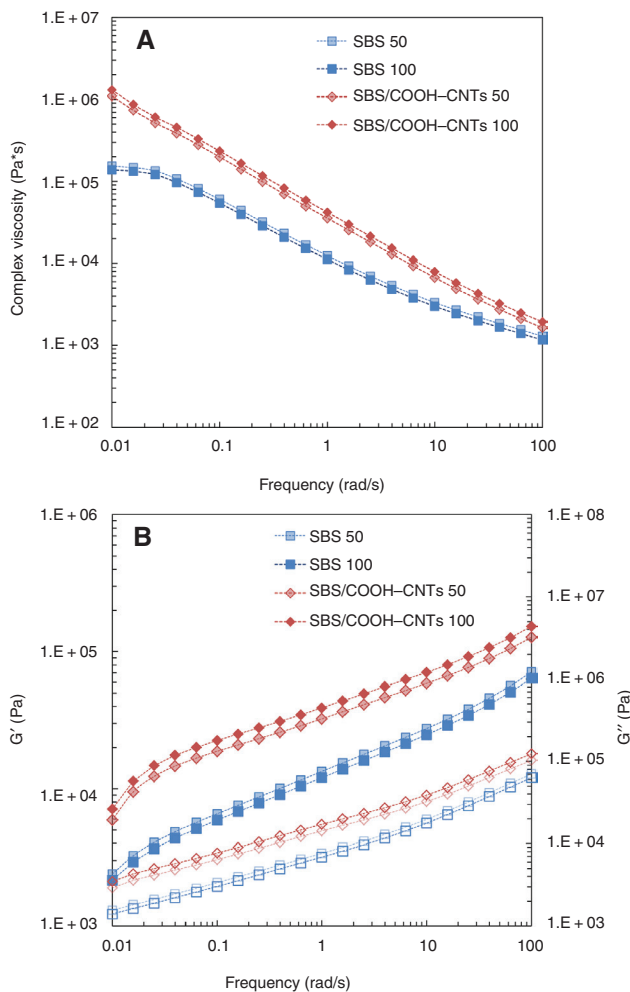


Figure 7: Complex viscosity and storage (full symbols) and loss (empty symbols) moduli as a function of frequency for neat SBS and SBS/COOH-CNTs nanocomposite at different mixing speeds.

the nanocomposite as a function of the mixing speed can be observed.

As far as the thermal properties of neat SBS and SBS/COOH-CNTs nanocomposite processed at 50 and 100 rpm are concerned, looking at the  $T_g$  values reported in Table 2 (Processing temperature 180°C, mixing speed 100 rpm), it is clearly observable that the variation of mixing speed has a negligible effect on the glass transition temperatures of both neat SBS copolymer and COOH-CNTs-containing nanocomposites.

In Figure 8E, the SEM micrograph of the SBS/COOH-CNTs nanocomposite processed at 100 rpm is reported. A homogeneous and uniform dispersion of functionalized CNTs within host matrix is noticeable, although no remarkable differences with respect to the morphology of the nanocomposite obtained at 50 rpm can be observed.

## 4 Conclusions

SBS/CNTs and SBS/COOH-CNT nanocomposites have been formulated through melt-mixing at different processing conditions with an aim to evaluate the influence of the processing temperature and of the mixing speed on the final properties of nanocomposites. Results coming from rheological and mechanical characterization clearly suggest that the overall properties of CNTs-containing nanocomposites progressively improve as the processing temperature increases, while no significant differences have been noticed as a function of mixing speed. The morphological analyses, performed to analyze the dispersion level of nanofillers within matrix and to evaluate

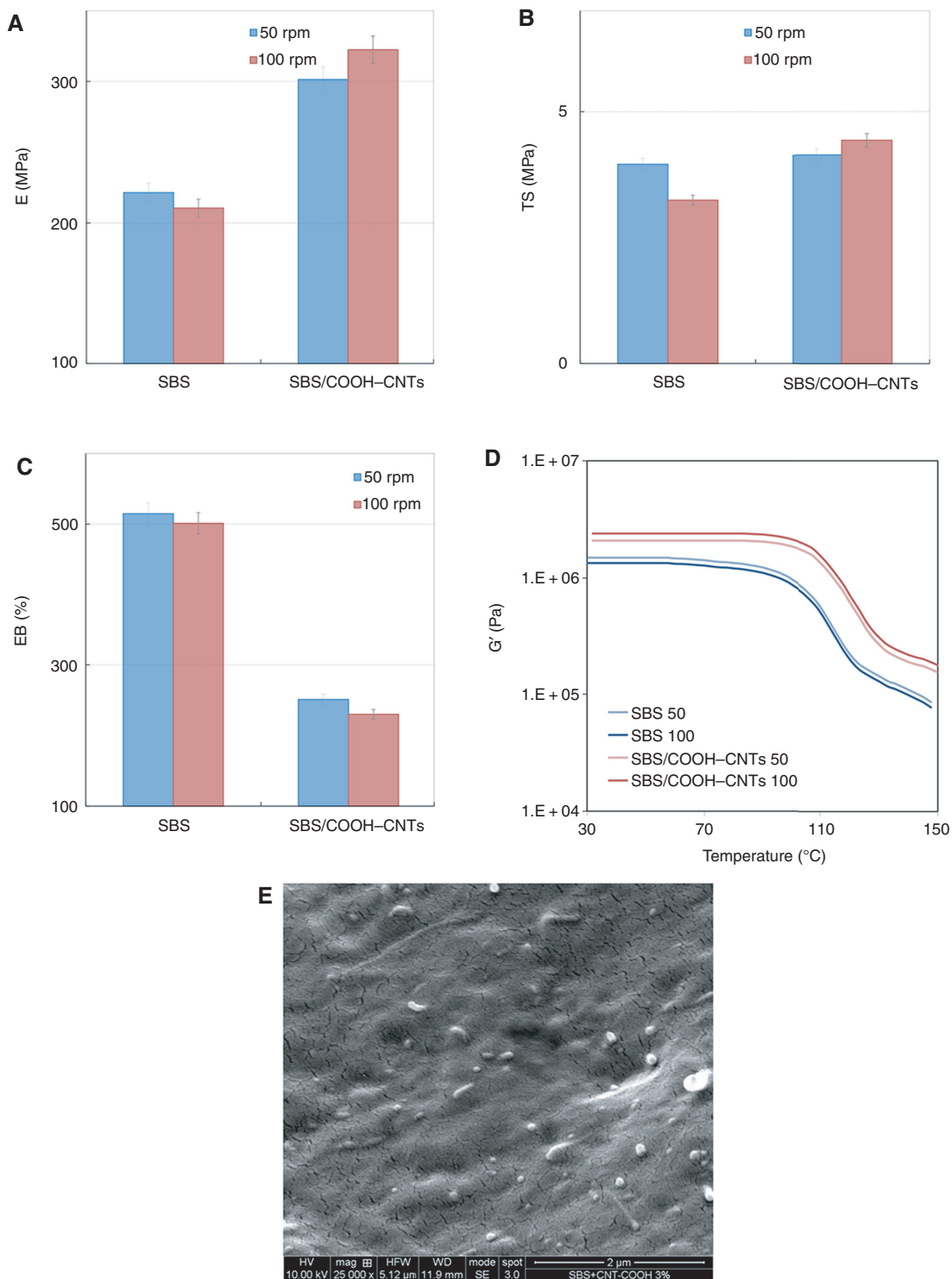


**Figure 8:** (A) Elastic modulus, (B) tensile strength, (C) elongation at break, (D) dynamic storage modulus for neat SBS and SBS/COOH-CNTs nanocomposite at different mixing speeds, and (E) SEM micrographs of SBS/COOH-CNTs nanocomposite obtained at high mixing speed.

the adhesion state between the CNTs and SBS copolymer, reveal that a uniform and homogeneous dispersion of both unmodified and -COOH functionalized CNTs has been achieved in the nanocomposites formulated at

180°C. Differently, at lower processing temperatures, a segregated morphology in which the nanofillers are selectively confined in the polybutadiene and/or polystyrene domains of the matrix has been obtained.

Overall, obtained results show that the processing temperature, more than mixing speed, has direct influence on the nanocomposites final properties, as the obtainment of a good state of dispersion of nanofillers within the host polymeric matrix strictly depends on the right choice of this parameter.

## References

- [1] Peddini SK, Bosniak CP, Henderson NM, Ellison CJ, Paul DR. *Polymer* 2015, 56, 443–451.
- [2] Lin L, Liu S, Zhang Q, Li X, Ji M, Deng H, Fu Q. *ACS Appl. Mater. Interf.* 2013, 5, 5815–5824.
- [3] Adhikari R, Michler GH. *Prog. Polym. Sci.* 2004, 29, 949–986.
- [4] Huy TA, Hai LH, Adhikari R, Weidisch R, Michler GH, Knoll K. *Polymer* 2003, 44, 1237–1245.
- [5] Sakurai S. *Trends Polym. Sci.* 1997, 5, 210–212.
- [6] Park C, Yoon J, Thomas EL. *Polymer* 2003, 44, 6725–6760.
- [7] Darling SB. *Progr. Polym. Sci.* 2007, 32, 1152–1204.
- [8] Huy TA, Adhikari R, Michler GH. *Polymer* 2003, 44, 1247–1257.
- [9] Holzer S, Ganß M, Schneider K, Knoll K, Weidisch R. *Eur. Polym. J.* 2013, 49, 261–269.
- [10] Li M, Tu W, Chen X, Wang H, Chen J. *J. Polym. Eng.* 2016, 36, 813–818.
- [11] Dintcheva NT, Arrigo R, Catalanotto F, Morici E. *Polym. Degr. Stab.* 2015, 118, 24–32.
- [12] Karabork F, Pehlivan E, Akdemir A. *J. Polym. Eng.* 2014, 34, 543–554.
- [13] Bockstaller MR, Mickiewicz RA, Thomas EL. *Adv. Mater.* 2005, 17, 1331–1349.
- [14] Albuerne J, Boschetti-de-Fierro A, Abetz C, Fierro D, Abetz V. *Adv. Eng. Mater.* 2011, 13, 803–810.
- [15] Peponi L, Valentini L, Torre L, Mondragon I, Kenny JM. *Carbon* 2009, 47, 2474–2480.
- [16] Peponi L, Tercjak A, Gutierrez J, Stadler H, Torre L, Kenny JM, Mondragon I. *Macromol. Mater. Eng.* 2008, 293, 568–573.
- [17] Park I, Lee W, Kim J, Park M, Lee H. *Sensor. Actuat. B Chem.* 2007, 126, 301–305.
- [18] Arrigo R, Morici E, Dintcheva NT. *Polym. Compos.* doi:10.1002/pc.23835 (In Press).
- [19] Pedroni LG, Araujo JR, Felisberti MI, Nogueira AF. *Compos. Sci. Technol.* 2021, 72, 1487–1492.
- [20] Tan QC, Shanks RA, Hui D, Kong I. *Compos. Part B Eng.* 2016, 90, 315–325.
- [21] Dintcheva NT, Morici E, Arrigo R, Zerillo G, Marona V, Sansotera M, Magagnin L, Navarrini W. *Compos. Part B Eng.* 2016, 95, 29–39.
- [22] Coleman JN, Khan U, Blau WJ, Gun'ko YK. *Carbon* 2006, 44, 1624–1652.
- [23] Dintcheva NT, Arrigo R, Nasillo G, Caponetti E, La Mantia FP. *J. Appl. Polym. Sci.* 2013, 129, 2479–2489.
- [24] Lu L, Zhou Z, Zhang Y, Wang S, Zhang Y. *Carbon* 2007, 45, 2624–2627.
- [25] Baibarac M, Baltog I, Lefrant S, Godon C, Mevellec JY. *Chem. Phys. Lett.* 2005, 406, 222–227.
- [26] Morici E, Arrigo R, Teresi R, Dintcheva NT. *AIP Conf. Proc.* 2016, 1736, 020030.
- [27] Arrigo R, Dintcheva NT, Guenzi M, Gambarotti C, Filippone G, Coiai S, Carroccio S. *Polym. Degr. Stab.* 2015, 115, 129–137.
- [28] Dintcheva NT, Arrigo R, Morici E, Gambarotti C, Carroccio S, Cicogna F, Filippone G. *Compos. Part B-Eng.* 2015, 82, 196–204.
- [29] Wang L, Wang Z, Wang Y, Wang X, Wang H, Lu G, Zhao D, Li Z. *J. Appl. Polym. Sci.* 2016, 133, 42945.
- [30] Dintcheva NT, Arrigo R, Gambarotti C, Carroccio S, Coiai S, Filippone G. *J. Appl. Polym. Sci.* 2015, 132, 42420.
- [31] Song YS, Youn JR. *Carbon* 2005, 43, 1378–1385.
- [32] Adedeji A, Grünfelder T, Bates FS, Macosko CW, Stroup-Gardiner M, Newcomb DE. *Polym. Eng. Sci.* 1996, 36, 1707–1723.
- [33] Zhang H, Yu J, Wang H, Xue L. *Mater. Chem. Phys.* 2011, 129, 769–776.
- [34] Canto LB, Torriani IL, Plivelic TS, Hage E, Pessan LA. *Polym. Int.* 2007, 56, 308–316.
- [35] Huegun A, Fernández M, Peña J, Muñoz ME, Santamaría A. *Nanomaterials* 2013, 3, 173–191.